Published in final edited form as:
Curr Biol. 2011 February 8; 21(3): 236–242. doi:10.1016/j.cub.2011.01.001.

Inter-tissue mechanical stress affects Frizzled-mediated planar cell polarity in the *Drosophila* notum epidermis

Patricio Olguín, **Alvaro Glavic**[*], and **Marek Mlodzik**[1]

Dept. of Developmental & Regenerative Biology, Mount Sinai School of Medicine, One Gustave L. Levy Place, New York, NY 10029

[*] Center for Genomics of the Cell, Faculty of Sciences, University of Chile, Las Encinas 3370, Santiago, Chile

Summary

Frizzled/Planar Cell Polarity (Fz/PCP) signaling controls the orientation of sensory bristles and cellular hairs (trichomes) along the antero-posterior axis of the *Drosophila* thorax (notum) [1–4]. A subset of the trichome-producing notum cells differentiate as “tendon cells”, serving as attachment sites for the indirect flight muscles (IFMs) to the exoskeleton [5]. Through the analysis of *chascon (chas)*, a gene identified by its ability to disrupt Fz/PCP signaling under overexpression conditions, and *jitterbug (jbug)/filamin* [6], we show that maintenance of antero-posterior planar polarization requires the notum epithelia to balance mechanical stress generated by the attachment of the IFMs. *chas* is expressed in notum tendon cells and its loss-of-function disturbs cellular orientation at and near the regions where IFMs attach to the epidermis. This effect is independent of the Fz/PCP and *fat (ft)/dachsous (ds)* systems [7]. The *chas* phenotype arises during normal shortening of the IFMs [8] and is suppressed by genetic ablation of the IFMs. *chas* acts through *jbug/filamin* and cooperates with MyosinII to modulate the mechano-response of notum tendon cells. These observations support the notion that the ability of epithelia to respond to mechanical stress generated by interaction(s) with other tissues during development/ organogenesis influences the maintenance of its shape and PCP features.

Results and Discussion

chascon is required to orient trichomes and bristles on the *Drosophila* notum

chascon (*chas*) was identified in an EP gain-of-function (GOF) screen for genes affecting wing morphogenesis [9]. *chas* encodes two isoforms, containing multiple predicted Src-homology and PDZ domain binding sites but no catalytic or conserved protein interaction domains, suggesting an adaptor or scaffold function (Figure S1 and not shown). Expression of either *chas* isoform in the posterior compartment of wing discs resulted in defects in cellular polarity, misplaced actin hair formation, and loss of asymmetric Fmi and Fz localization (Figure S1), suggesting that Chas can disturb PCP establishment and the localization of core Fz/PCP components [10]. *chas* GOF also displayed PCP defects in other tissues (e.g. ommatidial under-rotation in the eye, not shown). In the notum, Chas

[1]Author for correspondence: marek.mlodzik@mssm.edu, phone: 1-212-241 6516.

expression under *pannier-GAL4 (pnrG4*; expressed centrally in thorax, Fig. 1A) resulted in orientation and morphologic defects of bristles and trichomes (Figure 1B).

To ask whether *chas* is necessary for PCP and/or morphogenesis we generated UAS-dsRNA constructs targeting *chasA* (*chasAiR*) and used a VDRC UAS-dsRNA to a common exon (*chasABiR*) (Figure S1). *pnrG4* driven *chasABiR* or *chasAiR* resulted in notum bristles and trichomes pointing to the midline and multiple trichomes/cell (Figure 1C,F). Epidermal indentations were observed in most anterior notum regions (Figure 1C,F). As both dsRNAs showed indistinguishable phenotypes, we used *chasABiR* for subsequent studies. To confirm this, we generated a *chas* loss-of-function (LOF) allele (*chas*^{1}; via FLP-FRT deletion method [11]), lacking both 5′UTRs and start codons (Figure S1). *chas*^{1} animals were viable, fertile and displayed notal PCP and indentation defects similar to *pnrG4>chasABiR* (Figure 1E; no defects were observed in other tissues in *chas*^{1} or *chasABiR* animals). *chas*^{1}/Df, *tubG4>chasABiR*, and *chas*^{1} animals displayed similar defects, suggesting *chas*^{1} is a strong LOF or null allele (Figure S1). These LOF conditions exhibited weaker phenotypes than regional *dsRNA* gene knockdown or *chas*^{1} clones (Figure 1C,E–G,J; compare 1J medial domain with Figure S1), suggesting that differences in *chas* levels between mutant and adjacent wild-type tissue enhance polarity defects. *chas*^{1} defects were rescued by either Chas isoform in clones (MARCM[12]), confirming *chas*^{1} specificity (Figure S1). Furthermore, *chas*^{1} clones or regional knockdown influenced non-autonomously the orientation of wild-type cells, similar to *fz*- clones (Figure 1G–I; Figure S1).

chascon acts in parallel to the Fz/PCP-signaling

In the notum, Fz/PCP-signaling is required early to orient asymmetric divisions of SOPs and later to polarize cellular trichomes and bristle cells along the body axis (Figure S2) [2, 3, 13]. *chas* LOF did not affect the orientation of asymmetric SOP divisions (not shown). Thus *chas* appeared to act later, possibly interacting with Fz/PCP-signaling during PCP establishment in the notum epidermis (Figure S2). We explored the epistatic relationships between *chas* and Fz/PCP-core members. Strikingly, *chas*^{1}*;fz*^{p21} double mutants displayed a novel phenotype, with bristles and trichomes being reoriented towards the anterior (Figure 2A–C′,F; see Fig. S2 for related genotypes). These data suggested that *chas* and Fz/PCP-signaling work in parallel to polarize the notum epidermis.

As in other organs, the first signs of PCP in notal epidermal cells are asymmetric localizations of Fz/PCP-core components, evident from 24hAPF (hours after puparium formation) onwards (not shown) [10]. The localization/levels of Fz and Fmi were not affected in *pnrG4>chasABiR* animals at 30hAPF (Figure 2G–I′; compare with 2J–J′), further supporting the notion that *chas* and Fz/PCP-signaling act in parallel to promote PCP on the notum.

The *fat (ft)/dachsous (ds)* system controls PCP establishment in parallel to Fz/PCP-signaling [14], so we tested whether *chas* works through this system. The nota of strong *ds* combinations (*ds*^{38k}/*ds*^{UA071}), or *pnrG4* driven *ftiR*, *dsiR*, display bristles that are slightly oriented laterally (Figure 2D;Fig. S2), likely related to their mild thorax cleft and shape/size defects (consistent with role(s) in tissue growth and cell behavior [15]). Overall, the cleft and shape phenotypes associated with *ds*/*ft* LOF or GOF are not altered in *chas* LOF conditions, nor is the *chas* LOF phenotype (Figure 2D–F; Fig. S2 for details), suggesting that *chas* and the Fat/Ds-system act independently.

chascon preserves PCP and shape of the notum epithelium by modulating the mechanical properties of the tendon cells

chas LOF does not disturb asymmetric localizations of Fz/PCP-components, but still influences coordinated cell orientations in the notum. In *chas* LOF bristle and socket cells reorient polarity towards the midline between 30–32hAPF (Figure 3A–C; Movies S1–2), and epithelia displayed local cellular A/P contractions at the level of anterior dorsocentral macrochaetae (Figure 3A′–B′). This suggested that *chas* modulates the epithelial behavior at this stage to maintain PCP.

Most of trichome-producing cells of the notum differentiate as “tendon cells”, serving as attachment sites for indirect flight muscles (IFMs) (Figure S3) [5]. These cells form domains defined by *stripe* expression, which promotes tendon fate [8, 16]. IFMs start to shorten after 20hAPF, generating mechanical strain at attachment sites (Figure S3) [8]. This is evident in *dumpy* (*dp)* mutants, where notum epithelia are pulled inwards, resulting in epidermal indentations similar to *chas* mutants (Figure S3) [17, 18]. Dp, a transmembrane cuticular protein maintains the tension at muscle attachment sites by providing an anchor for cells to attach to the exoskeleton or modulating the cuticular matrix composition [18]. Double homozygous $chas^{1}$;dp^{ov1} animals showed stronger indentations and cell orientation defects than individual mutants (Figure S3), suggesting that *chas* is required to modulate mechanical properties of epidermal tendon cells during IFM shortening.

By 30hAPF *chas* expression was detected (via $chas^{NP0733G4}$ driven CD8-GFP staining; Figure S1) in tendon cells and was absent from socket and bristle cells (Figure S3). This was consistent with the *chas* LOF phenotype domains, supporting our genetic data that *chas* affects bristle polarity non-autonomously.

Subcellularly, Myc-tagged Chas localized at the apical cortex of tendon cells, colocalizing with E-Cadherin at adherent junctions, in tendon cell processes, and colocalizing with βPS-integrin at myotendinous junctions (Figure S3), consistent with a role of Chas linking the myotendinous junction and apical cortex.

Next, we monitored tendon cell processes and IFMs of live pupae expressing *chasABiR* and CD8-RFP under *pnrG4* and constitutively a GFP-Moesin fragment fusion (sGMCA) [19]. Anterior indentations were detected by 27–28hAPF and very obvious by 32hAPF, coinciding with attachment domains of ventral dorso-longitudinal muscles (DLMs), which are highly contracted at this stage (Figure 3D,G; Figure S3). Accordingly, the strongest bristle orientation defects in *chasABiR*, coincided with attachments of dorsal DLMs (Figure 3E,H). Tendon cell processes connecting DLMs in *chasABiR* did not elongate at 28–32hAPF, in contrast to wild-type, suggesting that tendons with reduced Chas levels respond differently to pulling stimuli (Figure S3). At 34–35hAPF, many cells formed multiple trichomes and oriented towards the midline (Figure 3F,I). This demonstrated that *chas* LOF defects arise during IFM shortening at DLM attachment domains and associate with elongation defects of epidermal tendon cells. The epithelial contraction of *pnrG4>chasABiR/ubi-DE-cadh-GFP* (Figure 3A–A′) coincided with posterior edges of the most dorsal DLM attachment domains, suggesting that pulling forces generated by muscle shortening alter the shape of these cells.

To confirm that IFMs were causing the cellular strain and defects in *chas* LOF cells, we eliminated the strain by ablating IFMs genetically via expressing activated Notch (N^{intra}) in muscle progenitors [20,21]. In this background, cellular orientation of $y,chas^{1}$ clones was almost completely rescued/suppressed (Figure 3J–K″). These data suggest that in tendons Chas balances pulling forces generated by IFM shortening to maintain shape and PCP of the notal epithelium.

The epidermal indentations in *chas* LOF arise at attachment sites of medial and ventral DLMs (Figure 3D), which form more perpendicular angles with the epithelial plane than dorsal DLMs [5]. This characteristic and our time-lapse studies suggested that the planar component of pulling forces transmitted through oblique attachments of dorsal DLMs impact directionally on the epithelial plane inducing a change of cellular orientation. The mechanical force, not compensated in *chas* mutant cells, is transmitted laterally, influencing mechanically the re-orientation of neighboring wild-type cells.

Of note, trichomes still localize to posterior cell edges in *chas* LOF, consistent with Fz/PCP-signaling still determining the position of trichome formation. When interfering with both, Fz/PCP-signaling and *chas*, the mechanical stress influences polarity stronger, leading to cellular orientation inverted anteriorly (Figure 2; Figure S2).

chascon acts through *jitterbug/filamin* and cooperates with *zipper/MyosinII*

To define *chas* function, we searched for genes displaying similar phenotypes within a genome-wide RNA-interference screen [22]. Knockdown of *jitterbug (jbug)* phenocopies all aspects of *chas* LOF (Figure 4A–B′). Co-expression of *jbugiR* and *chasiR* (under *pnrGal4*) showed an enhancement of polarity and indentation defects (Figure 4C–C′;Figure S4). *Jbug*, along with *cheerio*, encode the two *Drosophila* Filamin orthologs [6]. Filamins form homodimers that crosslink actin-filaments to confer mechanical stability to membranes [23]. They also work as molecular scaffolds linking transmembrane receptors with cytosolic signaling proteins and actin-filaments [23,24].

Whereas co-expression of *chasABiR* and *jbugiR* resulted in stronger defects than each dsRNAs separately (Figure 4C–C′; Figure S4), co-expression of wild-type JbugL isoform with *chasABiR* rescued *chas* LOF phenotypes (Figure 4D–D′; Figure S4). In contrast, Chas overexpression did not rescue *jbugiR* (not shown), suggesting that *jbug/Filamin* acts downstream of *chas*. Molecularly, Chas and Jbug proteins co-immunoprecipitated (Figure 4E), and co-localized with actin-filaments in S2R+ cells (not shown) and in tendon cells (Figure 4F), suggesting that they participate in a molecular complex associated with actin-filaments. These data suggest that *chas* acts through *jbug* to maintain shape and PCP of the notum.

Drosophila embryonic tendon cells contain prominent arrays of F-actin and MyosinII (MyoII), connecting the apical cortex with myotendinous junctions and maintaining the integrity of tendon cells upon stretching [25]. Rheological experiments have shown that actin-networks containing FilaminA display enhanced elasticity [26]. Accordingly, *chas* and *jbug* could modulate elastic properties of tendon cells, by regulating MyoII activity through small GTPases, its localization, or contributing in parallel to the formation and/or behavior of apico-basal F-actin networks.

We thus next analyzed localization of Zipper (Zip), *Drosophila* MyoII, and Shortstop (Shot), a Plakin that organizes apico-basal MT-networks in embryonic tendons [27]. Zip colocalizes partially with F-actin and Shot at tendon processes (Figure 4G). *chasABiR* did not disturb Zip or Shot localization/levels, suggesting that it is not required for F-actin/MyoII arrays or MT/Shot networks (Figure S4).

We knocked down Zip function at different pupal development stages via a dominant negative (*DN-zip*) under *pnrGal4* and *tubGal80ts* [28] (to bypass its cytokinesis role [29]). *DN-zip* expression from 0hAPF resulted in bristle orientation defects and epidermal indentations (Figure 4H;Figure S4). *DN-zip* or *chasABiR* expression at 14hAPF (18°C) resulted in weak orientation defects (Figure 4I,J;Figure S4). Strikingly, co-expression of *chasABiR* and *DN-zip* from 14hAPF caused strong PCP phenotypes and epidermal

indentations (Figure 4K). *chas* LOF phenotypes were not caused by diminished Zip activity, as expression of constitutively active *Drosophila* myosin regulatory light chain/MRLC (SqhE20E21) [30] did not rescue *chasABiR*-associated defects (not shown). This suggests that (1) *zip/MyoII* and *chas-jbug/filamin* cooperate to confer tendon cells with the ability to adapt to pulling forces generated by IFM shortening, and (2) the levels/activity of Filamin and MyoII regulate visco-elastic properties of actin-networks that run from myotendinous junctions to the apical cortex or at the apical cortex.

Conclusions

The notum epithelium develops in tight association with IFMs [5]. IFMs are directly attached to epithelial “tendon cells” and generate a pulling force over these cells [31] during PCP establishment. Mechanical properties of tendon cells and their interaction with muscles and the cuticle need to be finely tuned to maintain their shape and polarity [17,18]. Chas localizes from myotendinous junctions to the apical cortex and is upregulated during their maturation. Its function is likely to regulate Filamin activity/or localization to adjust elastic properties of tendon cells during IFM shortening. Since diminished MyoII activity mimics *jbug* or *chas* LOFs and tendon process length of *chasABiR* is not altered, we favor a role of Chas/Filamin in regulating elastic properties of F-actin arrays over length adaptation through active polymerization.

Mutations in Filamins are associated with human diseases, causing neuronal migration defects, bone and cartilage malformations, myopathies, and vascular defects, among others [23,24]. The role of Filamin in organogenesis/disease progression is in part related to its structural role modulating the visco-elastic properties of actin-filaments [24]. Our observations contribute to the understanding of the role(s) of Filamins as regulators of visco-elastic cellular properties during inter-tissue interactions. How does Chas modulate Filamin function? Since Chas does not present any catalytic domains, we favor the idea that it acts as an adaptor for Filamin. Thus, lack of *chas* may affect the composition/architecture of tendon actin-networks organized by Filamin.

In conclusion, we propose that *zip*/MyoII, *chas* and *jbug/filamin* have complementary roles in the apico-basal mechanical properties of tendon cells, influencing cytoskeletal dynamics at the apical cortex. Thus alterations in the ability to adjust to tensile forces operating in the apico-basal direction disrupt the epithelial shape, shift the site of trichome formation, their number per cell and their planar orientation. Our data reveal that interactions of two tissues and the ability of cells to adapt mechanically to them during morphogenesis are fundamental to maintain the shape and PCP of an epithelium.

Experimental procedures

See Supplemental Information.

Supplementary Material

Refer to Web version on PubMed Central for supplementary material.

Acknowledgments

We thank Hugo Bellen, Jose de Celis, Seth Blair, Kenneth Prehoda, Daniel Kiehart, Liqun Luo, Cristina Molnar, David Strutt, Talila Volk, Berkeley Drosophila Genome Project, VDRC, NIG-Fly, Exelixis/Harvard and the Bloomington center for flies and reagents; Sophy Okello, Joyce Lau, Ashok Ilankovan, Jaskirat Singh and Susana Franks for technical support; and David del Alamo, William Gault, Michel Gho, Ursula Weber, and Jun Wu for advice and discussion. This work was supported by NIH grant GM62917 to M.M., and ICM grant P06-039 to A.G. P.O. is a recipient of a postdoctoral fellowship from the Pew Latin American Fellows Program.

References

1. Gho M, Schweisguth F. Frizzled signalling controls orientation of asymmetric sense organ precursor cell divisions in Drosophila. Nature 1998;393:178–181. [PubMed: 9603522]
2. Krasnow RE, Adler PN. A single frizzled protein has a dual function in tissue polarity. Development 1994;120:1883–1893. [PubMed: 7924994]
3. Bellaiche Y, Beaudoin-Massiani O, Stuttem I, Schweisguth F. The planar cell polarity protein Strabismus promotes Pins anterior localization during asymmetric division of sensory organ precursor cells in Drosophila. Development 2004;131:469–478. [PubMed: 14701683]
4. Lu B, Usui T, Uemura T, Jan L, Jan YN. Flamingo controls the planar polarity of sensory bristles and asymmetric division of sensory organ precursors in Drosophila. Curr Biol 1999;9:1247–1250. [PubMed: 10556092]
5. Bate, M. The mesoderm and its derivatives. In: Bate, M.; Martinez Arias, A., editors. The development of Drosophila Melanogaster. Vol. II. New York: Cold Spring Harbor Laboratory Press; 1993. p. 1059-1078.
6. Brown NH, Gregory SL, Martin-Bermudo MD. Integrins as mediators of morphogenesis in Drosophila. Dev Biol 2000;223:1–16. [PubMed: 10864456]
7. Lawrence PA, Struhl G, Casal J. Planar cell polarity: one or two pathways? Nat Rev Genet 2007;8:555–563. [PubMed: 17563758]
8. Sandstrom DJ, Restifo LL. Epidermal tendon cells require Broad Complex function for correct attachment of the indirect flight muscles in Drosophila melanogaster. J Cell Sci 1999;112(Pt 22): 4051–4065. [PubMed: 10547365]
9. Molnar C, Lopez-Varea A, Hernandez R, de Celis JF. A gain-of-function screen identifying genes required for vein formation in the Drosophila melanogaster wing. Genetics 2006;174:1635–1659. [PubMed: 16980395]
10. Seifert JR, Mlodzik M. Frizzled/PCP signalling: a conserved mechanism regulating cell polarity and directed motility. Nat Rev Genet 2007;8:126–138. [PubMed: 17230199]
11. Parks AL, Cook KR, Belvin M, Dompe NA, Fawcett R, Huppert K, Tan LR, Winter CG, Bogart KP, Deal JE, et al. Systematic generation of high-resolution deletion coverage of the Drosophila melanogaster genome. Nat Genet 2004;36:288–292. [PubMed: 14981519]
12. Lee T, Luo L. Mosaic analysis with a repressible cell marker (MARCM) for Drosophila neural development. Trends Neurosci 2001;24:251–254. [PubMed: 11311363]
13. Gho M, Bellaiche Y, Schweisguth F. Revisiting the Drosophila microchaete lineage: a novel intrinsically asymmetric cell division generates a glial cell. Development 1999;126:3573–3584. [PubMed: 10409503]
14. Casal J, Lawrence PA, Struhl G. Two separate molecular systems, Dachsous/Fat and Starry night/ Frizzled, act independently to confer planar cell polarity. Development 2006;133:4561–4572. [PubMed: 17075008]
15. Aigouy B, Farhadifar R, Staple DB, Sagner A, Roper JC, Julicher F, Eaton S. Cell flow reorients the axis of planar polarity in the wing epithelium of Drosophila. Cell 2010;142:773–786. [PubMed: 20813263]
16. Fernandes JJ, Celniker SE, VijayRaghavan K. Development of the indirect flight muscle attachment sites in Drosophila: role of the PS integrins and the stripe gene. Dev Biol 1996;176:166–184. [PubMed: 8660859]
17. Metcalfe JA. Developmental genetics of thoracic abnormalities of dumpy mutants of Drosophila melanogaster. Genetics 1970;65:627–654. [PubMed: 5518509]
18. Wilkin MB, Becker MN, Mulvey D, Phan I, Chao A, Cooper K, Chung HJ, Campbell ID, Baron M, MacIntyre R. Drosophila dumpy is a gigantic extracellular protein required to maintain tension at epidermal-cuticle attachment sites. Curr Biol 2000;10:559–567. [PubMed: 10837220]
19. Kiehart DP, Galbraith CG, Edwards KA, Rickoll WL, Montague RA. Multiple forces contribute to cell sheet morphogenesis for dorsal closure in Drosophila. J Cell Biol 2000;149:471–490. [PubMed: 10769037]

20. Bernard F, Dutriaux A, Silber J, Lalouette A. Notch pathway repression by vestigial is required to promote indirect flight muscle differentiation in Drosophila melanogaster. Dev Biol 2006;295:164–177. [PubMed: 16643882]
21. Go MJ, Eastman DS, Artavanis-Tsakonas S. Cell proliferation control by Notch signaling in Drosophila development. Development 1998;125:2031–2040. [PubMed: 9570768]
22. Mummery-Widmer JL, Yamazaki M, Stoeger T, Novatchkova M, Bhalerao S, Chen D, Dietzl G, Dickson BJ, Knoblich JA. Genome-wide analysis of Notch signalling in Drosophila by transgenic RNAi. Nature 2009;458:987–992. [PubMed: 19363474]
23. Stossel TP, Condeelis J, Cooley L, Hartwig JH, Noegel A, Schleicher M, Shapiro SS. Filamins as integrators of cell mechanics and signalling. Nat Rev Mol Cell Biol 2001;2:138–145. [PubMed: 11252955]
24. Zhou AX, Hartwig JH, Akyurek LM. Filamins in cell signaling, transcription and organ development. Trends Cell Biol.
25. Alves-Silva J, Hahn I, Huber O, Mende M, Reissaus A, Prokop A. Prominent actin fiber arrays in Drosophila tendon cells represent architectural elements different from stress fibers. Mol Biol Cell 2008;19:4287–4297. [PubMed: 18667532]
26. Gardel ML, Nakamura F, Hartwig J, Crocker JC, Stossel TP, Weitz DA. Stress-dependent elasticity of composite actin networks as a model for cell behavior. Phys Rev Lett 2006;96:088102. [PubMed: 16606229]
27. Subramanian A, Prokop A, Yamamoto M, Sugimura K, Uemura T, Betschinger J, Knoblich JA, Volk T. Shortstop recruits EB1/APC1 and promotes microtubule assembly at the muscle-tendon junction. Curr Biol 2003;13:1086–1095. [PubMed: 12842007]
28. Franke JD, Montague RA, Kiehart DP. Nonmuscle myosin II generates forces that transmit tension and drive contraction in multiple tissues during dorsal closure. Curr Biol 2005;15:2208–2221. [PubMed: 16360683]
29. Murthy K, Wadsworth P. Myosin-II-dependent localization and dynamics of F-actin during cytokinesis. Curr Biol 2005;15:724–731. [PubMed: 15854904]
30. Winter CG, Wang B, Ballew A, Royou A, Karess R, Axelrod JD, Luo L. Drosophila Rho-associated kinase (Drok) links Frizzled-mediated planar cell polarity signaling to the actin cytoskeleton. Cell 2001;105:81–91. [PubMed: 11301004]
31. Sandstrom DJ, Bayer CA, Fristrom JW, Restifo LL. Broad-complex transcription factors regulate thoracic muscle attachment in Drosophila. Dev Biol 1997;181:168–185. [PubMed: 9013928]

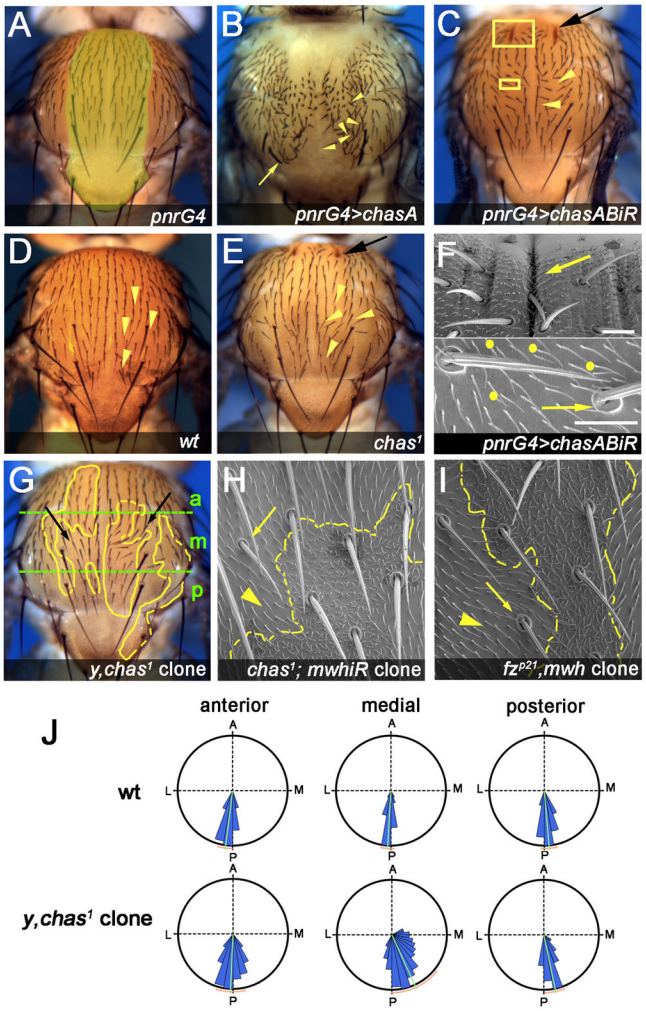

Figure 1. *chas* is required to orient bristles and trichomes in the notum

(A–I) All panels show dorsal views of nota (dorsal thorax), oriented with anterior to the top in this and all following figures.

(A) Control notum (*pnrG4)*, the *pnr* expression domain is indicated in yellow.

(B) *pnrG4>UAS-chasA*: Note mild thorax cleft, bristle polarity (arrowheads) and bristle morphology defects (arrow).

(C, F) *pnrG4>chasABiR*. In (C) yellow boxes represent the areas magnified in F. Note that bristles (C and F bottom), socket cells (F bottom, arrow) and cellular trichomes are oriented towards the midline (right in F bottom). Indentations of the epidermis are marked (C, F top, black and yellow arrows). Yellow dots indicate cells with multiple trichomes (F, bottom). Note that PCP defects are stronger between the anterior suture and dorsocentral macrochaetae (C). Bars 20 μm.

(E) *chas*^{1} displays polarity (arrowhead) and indentation defects (arrow); compare to wild-type control in (D).

(G–J) *chas*^{1} clones, marked with *yellow* (*y* in G) or *multiple wing hairs* (*mwh* in H), non-autonomously influence the polarity of neighboring bristles (G) and cells/trichomes (H). Clone boundaries are outlined in yellow. Note that the *chas*^{1} non-autonomous effects are similar albeit weaker to *fz* loss of function clones (compare H and I). (J) Quantitative analysis of *chas*^{1} mitotic clones (marked with *yellow*) represented in polar charts. The mean and standard deviation are indicated with a green and orange line respectively. Each notum

was divided into three sectors (anterior/a, middle/m and posterior/p: for an example see panel [G], green lines). The angles of mutant bristles were measured with respect to the midline (0°) and compared with wild-type bristles in the same sector (black). Bristle orientation is significantly biased towards the midline in all sectors. Note that *chas*^{1} bristles at the middle sector display the strongest orientation defects and the largest increment of the standard deviation (mean +/− SD: 25.66 +/− 28.19°, n=699) comparing to the control (−3.321 +/− 7.342°, n=146). A very similar or identical measurement was performed for all genotypes analyzed in this study, see Figure S1 for more graphs.

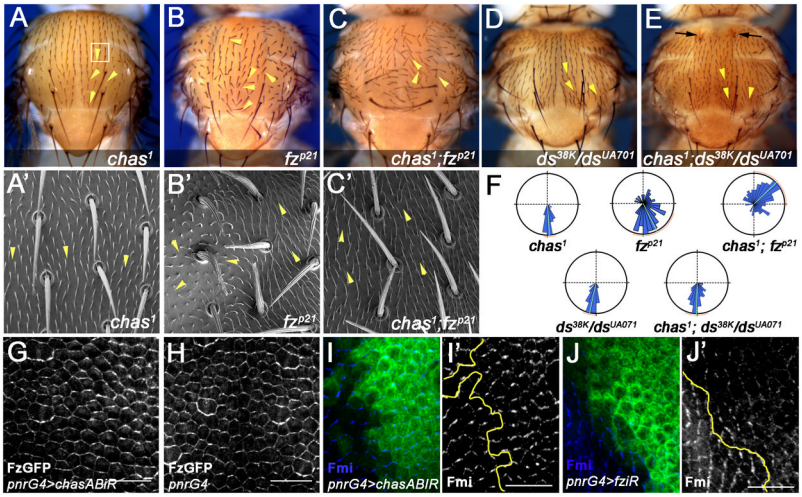

Figure 2. *chas* and the Fz/PCP signaling pathway act in parallel to orient bristles and trichomes on the notum

Panels A–E show dorsal views of adult nota, with anterior up.

(A, A′) *chas*^{1} male, white square represents the region showed in high magnification of this and other genotypes in panels A′ to C′. (B, B′) *fz* null males (*fz*^{p21}): Note that the orientation of trichomes is randomized in the central region (left) compared with the lateral one (right, arrowheads in B′). (C, C′) Double mutants *chas*^{1}*; fz*^{p21}: note an enhancement of the PCP orientation defects of bristles and trichomes and reorientation towards the anterior (indicated by arrowheads in C′). See quantitative analysis in (F)

(D–E) Nota of *ds*^{38k}/*ds*^{UA071} (D) and double mutant *chas*^{1}*; ds*^{38k}/*ds*^{UA071} (E). The bristle orientation of *chas*^{1}*; ds*^{38k}/*ds*^{UA07} flies (E, arrowheads) appears to be a combination of both phenotypes (E–F). Note the enhancement of the indentation defect (E, arrows).

(G–J′) 30hAPF Pupal nota labeled with Fz-GFP (G–H) or antibodies (I–J′) as indicated.

(G–H) Nota labeled with Fz-GFP of *pnrG4*, *UAS-chasABiR* and the wild-type control (*pnrG4*).

(G). Note that the Fz-GFP pattern is not affected by the *chasABiR* gene knock-down.

(I–J′) Nota stained for Fmi (blue and monochrome in I′ and J′), *pnr*-domain is marked with GFP (green in I, J) and its edge indicated with yellow lines (I′, J′). (J, J′) *pnrG4>fziR* shows diminished levels of Fmi and non-autonomous reorientation of its localization along the anterior posterior axis. In contrast, *pnrG4>chasABir* (I–I′) does not affect Fmi localization (compare also with G) or orientation at anterior-posterior cell boundaries. Bar 30 μm. See also Figure S3 and S4.

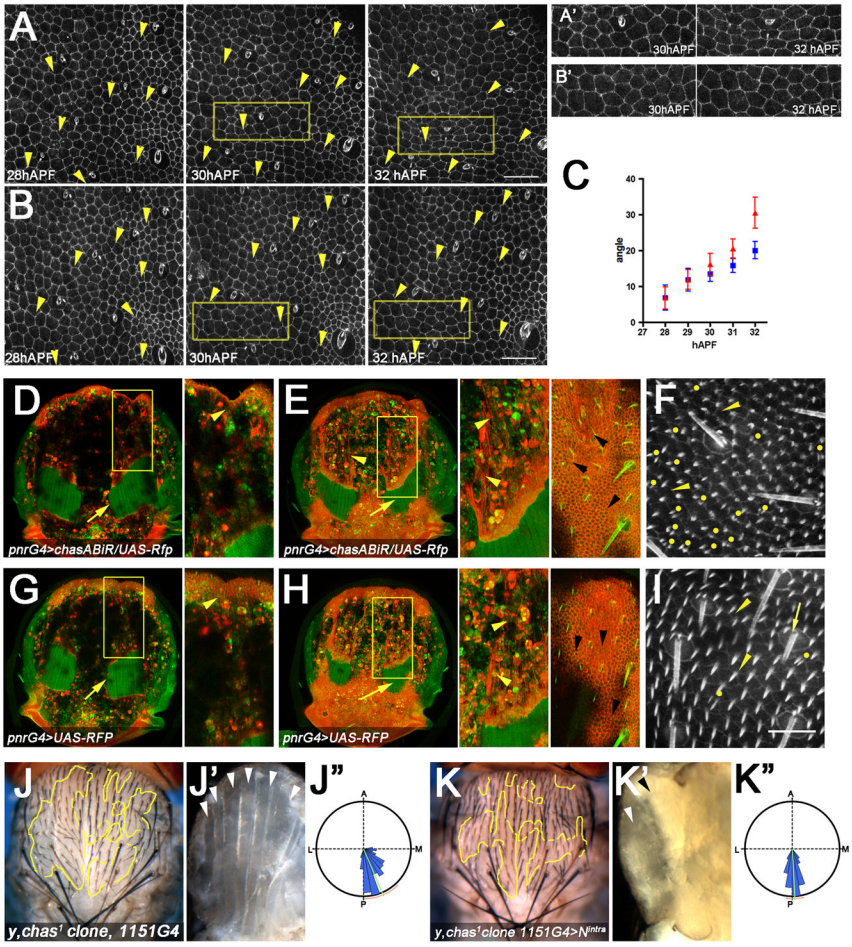

Figure 3. *chascon* preserves the PCP and shape of the notum epithelium by modulating the mechanical properties of the tendon cells

(A–B) Time-lapse sequence of notum epithelium highlighted with *ubi-DE-cadh-GFP* at the level of the adherent junctions from 28 to 32 hAPF. The dorsocentral macrochaetae was used as a positional reference at the bottom right of the images. Anterior is up and medial to the left.

(A) The orientation of *pnrG4>chasABiR* bristle and socket cells (arrowheads) rotate towards the midline more than the control (*pnrG4*) (B).

(C) Quantitative analysis of the bristle and socket cells angles with respect to the midline at different time points. Note that at 32 hAPF the average angle of *pnrG4>chasABiR* bristle and socket cells is significantly larger (mean±SEM = 30.53 ± 4.335, n=22) than the control (20.04 ± 2.371, n=26) (p=0.0321).

(A′, B′) Magnified views of the notum region indicated with yellow squares in A and B. Note the contraction of the *pnrG4>chasABiR* epithelium (A′) during the time (compare with B′, control). See also Suppl. Movie1 and 2.

(D, E, G, H) Live nota at 32 hAPF labeled with CD8-RFP (red) in the *pnr* domain and constitutively expressing Moesin-GFP (green). Note the tendon processes in red (arrowheads E and H) and the DLMs in green (arrows).

(D, G) Tangential confocal projections (12μm) of nota at the level of medial and ventral DLMs. Anterior indentations are evident in *pnrG4>chasABiR* (D, arrowheads, cf. with G, insets).

(E, H) Tangential confocal projections (12 μm) of nota showing the most dorsal DLMs and tendon processes located right below the epithelium (right detailed view). Note that tendon cell processes (arrowheads, left detailed view) coincide with the orientation defects of *pnrG4>chasABiR* at the epithelium (arrowheads, right detailed view). Compare with control (*pnrG4*) (H).
(F, I) Nota at 35 hAPF labeled with Moesin-GFP (sGMCA). Confocal images at the level of the apical side of the notum epithelial cells showing bristle, socket (arrows) and trichome orientation (arrowheads). (F) *pnrG4>chasABiR* leads to many cells forming multiple trichomes (marked by yellow dots) at central-lateral domains of the notum as compared to the control (I). Bar 30 μm.
(J–K″) Genetic ablation of DLMs suppresses $chas^{1}$ orientation defects.
(J, K) Adult notum showing *y*, $chas^{1}$ clones in combination with the imaginal muscle progenitor cells driver *1151G4.* (K) $chas^{1}$ orientation phenotype is suppressed in the $1151G4>N^{intra}$ background, compare with control (J). (J″, K″) Quantitative analysis compare J″ (mean +/− SD: 23.65 +/− 21.82, n=233) with K″ (2.85 +/− 11.31, n= 130).
(J′, K′) Note the absence of DLMs in the $chas^{1}$, $1151G4>N^{intra}$ flies (K′) compared with the control (J′, arrowheads).

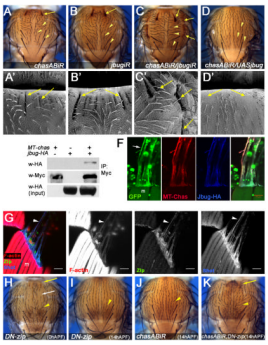

Figure 4. *chas* regulates *jbug/filamin* and cooperates with *zipper/MyosinII* to maintain the shape and PCP of the notum epithelia

Panels A–D′ show nota from the genotypes indicated, anterior is up.

(A–B″) *pnrG4>jbugiR* (B–B″) nota display similar anterior indentation of the cuticle/epidermis (compare A, A′ with B, B′, arrows) and PCP phenotypes to *pnrG4>chasABiR* (compare A with B, arrowheads). (C–C′) Double knockdown condition *pnrG4>chasABiR, jbugiR*, shows enhanced indentation (C, C′, arrows) and PCP defects (C, arrowheads). Note that additional lateral indentations arise in this genetic background (C, C′). (D–D″) Overexpression of *jbug* (JbugL: the isoform comprises an amino-terminal actin-binding domain and seven Filamin-type IG-domains and does not cause dominant effects in the notum or other epithelia) rescues the PCP (D, arrowheads) and indentation defects (D′, arrows) associated with a *chas* knockdown, suggesting that Jbug/Filamin is regulated by Chas.

(E) Myc-tagged(MT)-Chas and Jbug-HA co-immunoprecipitate. Protein extracts from S2R+ cells transfected with MT-Chas and/or Jbug-HA (as indicated on top) were immunoprecipitated with an anti-Myc antibody. The corresponding extracts were analyzed by Western-blot with anti-HA (upper panel) and anti-Myc (middle panel). The lower panel shows input analyzed with anti-HA. Note that Jbug-HA is detected only in the extract corresponding to the cells co-transfected with MT-Chas and Jbug-HA.

(F) Tendon cell processes corresponding to a Flip-out clone expressing *GFP*, *UAS-MT-chas* and *UAS-jbug-HA*. Note that *Myc-Chas* (MT-Chas; red) and Jbug-HA (blue) colocalize at 27 hAPF. Bar 20 μm.

(G) Confocal projection of DLMs and the myotendinous junction at 33 hAPF.

(A) Control labeled with phalloidin (red), Zip (green) and Shot (blue). Note that tendon projections are enriched in F-actin, Shot and Zip (arrowheads). Bar 20 μm.

(H–K) Expression of *DN-zip* and/or *chasABiR* at different stages of pupal development using *pnrG4* and *tubulin>Gal80ts*. (H) Early induction (0 hAPF) results in indentations (arrow), bristle orientation/PCP defects (yellow arrowhead) and loss of bristles probably due to cytokinesis defects (white arrow). (I) Late expression of *DN-zip* (14 hAPF) alters the orientation of bristles similarly to late *chasABiR* expression (compare to J) (yellow arrowheads). Note that expression of *DN-zip* from this stage onward does not affect bristle number or spacing (compare H and I). (K) Late coexpression of *DN-zip* and *chasABiR* (14 hAPF) results in stronger orientation/PCP defects (arrowheads) and in anterior indentations (arrow).